Comparative analysis of drag force of two train models

Szymon Górski[1], Patryk Peret[2]

[1]*Cracow University of Technology, Department of Mechanical Engineering, Institute of Thermal and Process Engineering,al. Jana Pawła II 37, 31-864 Cracow, Poland*

[2]*Cracow University of Technology, Department of Mechanical Engineering, Institute of Thermal Power Engineering, al. Jana Pawła II 37, 31-864 Cracow, Poland*

Abstract

The purpose of presented work is the aerodynamic comparison, especially the generated drag force, of the two train models used in Poland. Another thing is the comparison of the resulting drag force for different turbulence models used in the CFD calculations. 3D geometries based on the real dimensions of Pendolino ED250 and Impuls 45WE trains are created in Autodesk Inventor. Numerical flow analysis are carried out in the Ansys Fluent software. This analysis contain comparison of the basic flow parameters and influence of mesh on the results.

*Keywords:*CFD; turbulence models; numerical modelling;drag force; aerodynamic comparison;

1.Introduction

Nowadays numerical modelling become a common tool for engineers because they can predict what will happen in the future or optimise shape of designing part by one or more parameters. CFD calculations can be used in every kind of engineering sciences for example to compute the drag force.This numerical analysis shows answer which of two trains generate less drag force value than the second one.

Selected turbulence models for comparative analysis:

I. Spalart-Allmaras models[1]:

- Vorticity-based production,
- Strain/ Vorticity-based production,

II. k-ε models:

- Standard [2],
- RNG [3],
- Realizable[4],

II. k-ω models:

- Standard [5],
- SST [6].

Second part includes influence of mesh on the results in order to prove the importance of boundary layer. Finally, this work presents a relationship between drag force and train velocity for both 3D models on graphs.

2. Turbulence models

Turbulent flows are characterized by fluctuating velocity fields. These fluctuations mix transported quantities such as momentum, energy, and species concentration, and cause the transported quantities to fluctuate as well. Instead, the instantaneous (exact) governing equations can be time-averaged, ensemble-averaged, or otherwise manipulated to remove the small scales, resulting in a modified set of equations that are computationally easy solve. However, the modified equations contain additional unknown variables, and turbulence models are needed to determine these variables in terms of known quantities. The Reynolds-number of a flow gives the measure of relative inertia forces and viscous forces. At values of the Reynolds numbers above critical Reynolds number, the fluid flow is called turbulent flow with random and chaotic behavior. There are complicated series of events which eventually leads to change of the flow character.

2.1. Spalart-Allmaras model theory

The Spalart-Allmaras model is one-equation model that solves a transport equation for a quantity that is a modified form of the turbulent kinematic viscosity. This model was specifically designed for aerospace and turbomachinery applications involving wall-bounded flows and has been shown to give good results for boundary layers subjected to adverse pressure gradients. The Spalart-Allmaras model has been implemented to use wall functions when the mesh resolution is not sufficiently fine despite of this that it is low-Reynolds-number model. This might make it the best choice for relatively crude simulations on coarse meshes. The biggest drawback is that this model has inability to rapidly accommodate changes in length scale[1].

2.2. k-ε models theory

All models which are counted to this theory have similar formulas based on transport equations for turbulent kinetic energy (k) and rate of viscous dissipation (ε). The main distinction in the models are as follows[2]:

- the method of calculating turbulent viscosity,
- the turbulent Prandtl numbers governing the turbulent diffusion of k and ε,
- the generation and destruction terms in the ε equation.

*Corresponding author: szygor9907@gmail.com; patryk.peret@interia.pl

The model transport equation for k is derived from the exact equation, while the model transport equation for ε was obtained using physical reasoning.

Major assumptions in the derivation of k-ε [2]:

- the flow is fully turbulent,
- effects molecular viscosity are negligible.

Each model has basically the same qualities: turbulent production, buoyancy force, figure effects of compressibility.Transport equations for k and ε consist:

- the generation of turbulence kinetic energy due to the mean of velocity gradient – G_k,
- the generation of turbulence kinetic energy due to buoyancy – G_b,
- the contribution of the fluctuating dilatation in compressible turbulence to the overall dissipation rate – Y_M,
- the turbulent Prandtl numbers for k and ε – σ_k and σ_ε,
- constant values – $C_{1\varepsilon}$, $C_{2\varepsilon}$, $C_{3\varepsilon}$ and C_μ,
- user-defined source terms – $S_k$and S_ε.

Table 1.*Constant values and turbulent Prandtl numbers for k-ε models [2],[3],[4].*

Symbol	standard k-ε model	RNG k-ε model	realisable k-ε model
$C_{1\varepsilon}$	1.44	1.42	1.44
$C_{2\varepsilon}$	1.92	1.68	1.9
C_μ	0.09	0.08 45	variable
σ_k	1.0	0.7194	1.0
σ_ε	1.3	0.7194	1.2

2.2.1. Standard k-ε model

This "complete" semi-empirical model of turbulence is two-equation model with two separate transport equations, which it was proposed by Launder and Spalding in 1972. This model is used commonly in industrial flow and heat transfer simulation, because of robustness, economy and reasonable accuracy.When advantages and disadvantages of this model have become known then engineers improvedits performance by devising another two variants [2].

2.2.2. RNG k-ε model

The first refined k-ε model is using a rigorous statistical technique,which is called renormalization group theory. This model has an additional term in its ε equation that significantly improves the accuracy for rapidly strained flows. The effect of swirl on turbulence is included in the RNG model, enhancing accuracy for swirling flows.The RNG theory provides an analytical formula for turbulent Prandtl numbers, while the standard k-ε model uses user-specified, constant values.While the standard k-ε model is a high-Reynolds-number model, the RNG theory provides an analytically-derived differential formula for effective viscosity that accounts for low-Reynolds-number effects. Effective use of this feature does, however, depend on an appropriate treatment of the near-wall region.This model is derived from the instantaneous Navier-Stokes equations [3].

2.2.3. Realisable k-ε model

The realisable k-ε model differs from standard k-ε model, because this model contains a new formulation for the turbulent viscosity. A new transport equation for the dissipation rate has been derived from an exact equation for the transport of the mean-square vorticity fluctuation. The term "realizable" means that the model satisfies certain mathematical constraints on the Reynolds stresses, consistent with the physics of turbulent flows [4]. Initial studies have shown that the realizable model provides the best performance of all the k-ε model versions for several validations of separated flows and flows with complex secondary flow features.One limitation of this model is that it produces non-physical turbulent viscosities in situations when the computational domain contains both rotating and stationary fluid zones. A new eddy-viscosity formula involving a variableC_μ originally proposed by Reynolds.

2.3. k-ω models theory

Both models goes on transport equations for turbulent kinetic energy (k) and turbulence frequency (ω). The turbulence frequency is the ratio of turbulence dissipation ratio to turbulent kinetic energy and this relationship is given by undermentioned formula [5]:

$$\omega = \frac{\varepsilon}{k}, \tag{1}$$

ω turbulence frequency (1/s),
ε turbulence dissipation rate (m^2/s^3),
k turbulent kinetic energy (m^2/s^2).

The main difference between the SST model and the standard model are:

- gradual change from the standard k-ω model in the inner region of the boundary layer to a high-Reynolds-number version of the k-ε model in the outer part of the boundary layer,
- modified turbulent viscosity formulation to account for the transport effects of the principal turbulent shear stress.

Transport equations for k and ω incorporate:

- the generation of turbulence kinetic energy due to the mean of velocity gradient – G_k,
- the generation of turbulence frequency – G_ω,
- the effective diffusivity – Γ_k and Γ_ω,
- the dissipation due to turbulence – Y_k and Y_ω,
- user-defined source terms – S_k and S_ω.

2.3.1. Standard k-ω model

The standard Wilcox model was developed and allows for low-Reynolds-number effects, compressibility and shear flow spreading, which is an empirical model. This model is applied for wall-bounded flows and free shear flows [5].

2.3.2. SSTk-ω model

The SST k-ω model is based on both the standard k-ω model and the standard k-ε model and this introduce the definition of shear stress turbulence. This model couple conveniences from both models by using blending function. The damp cross-diffusion derivative term is used in transport equations. This model has application in wider class of flows, for example transonic shock waves or airflow pressure [6].

2.4. Parameters of airflow

The main parameters, which were used for aerodynamic comparison in this paper are defined in this chapter.

2.4.1. Drag force

The basic formula for drag force (D) is presented by this equation:

$$D = P_d \cdot C_d \cdot A, \tag{2}$$

D drag force (N),
P_d dynamic pressure (N/m^2),
A reference area (m^2),
C_d drag coefficient (-).

The drag coefficient depends on the shape of obstacle and Reynolds-number. Thus drag force is proportional to fluid density and second power of velocity, because of following formula for dynamic pressure:

$$P_d = \frac{1}{2} \cdot \rho \cdot v^2, \tag{3}$$

P_d dynamic pressure (N/m^2),
ρ fluid density (kg/m^3),
v flow velocity relative to the object (m/s).

2.4.2. Turbulence intensity

The turbulence intensity is defined as the ratio between root-mean-square of the turbulent velocity fluctuation and Reynolds average velocity:

$$I = \frac{u`}{U} = \frac{\sqrt{\frac{2}{3}k}}{\sqrt{U_x^2+U_y^2+U_z^2}}, \tag{4}$$

I turbulence intensity (-),
$u`$ turbulent velocity fluctuation (m/s),
U mean velocity (m/s),
U_x, U_y, U_z mean velocity components (m/s),
k turbulent kinetic energy (m^2/s^2).

2.4.3. Turbulent viscosity ratio

The eddy viscosity ratio shows the relationship between the turbulent viscosity and the molecular dynamic viscosity.

3. Preprocessing and results

The definition of the geometry, grid generation, fluid properties and the specification of boundary conditions were set up in preprocessor to start the simulation. The second part of this chapter presents a solution for different types of turbulence models and discretisation methods. The CFD analysis results are shown in figures.

3.1. 3D geometries

Geometries of two trains: Pendolino ED250 and Impuls 45WE were created in Autodesk Inventor and are based on real dimensions of their height and width. The length of trains is similar because flow parameters are compared with respect to the front and rear train shapes. Domain geometry of trains and train sizes are presented in table 2 and 1. The computational domains are cuboids. Train models are simplified.

Table 2.*Dimensions of computational domains.*

Name of train	Length (mm)	Width (mm)	Height (mm)
Pendolino ED250	130000	9 000	10 400
Impuls 45WE	130000	9 000	10 400

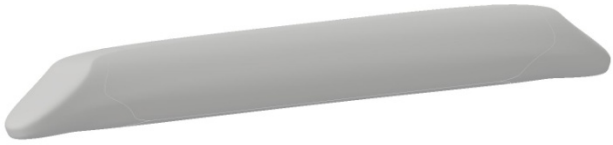

Figure 1. *3D geometry of Pendolino ED250.*

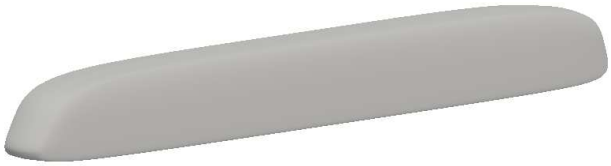

Figure 2. *3D geometry of Impuls 45WE.*

Table 3.*Dimensions of train geometries.*

Name of train	Length (mm)	Width (mm)	Height (mm)
Pendolino ED250	60 000	2 830	4 100
Impuls 45WE	60 000	2 840	4 150

3.2. Mesh statistics

The subdivision of the domain was generated in Mesh module of Ansys software. In both cases finite elements have maximum face size sets on 300 (mm) and 3 layers of inflation around trains with growth rate equals 1.2.

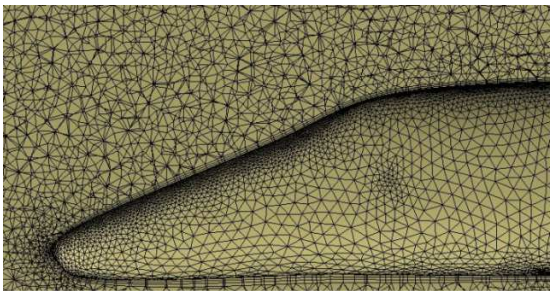

Figure 3. *Grid generated, front of the Pendolino train.*

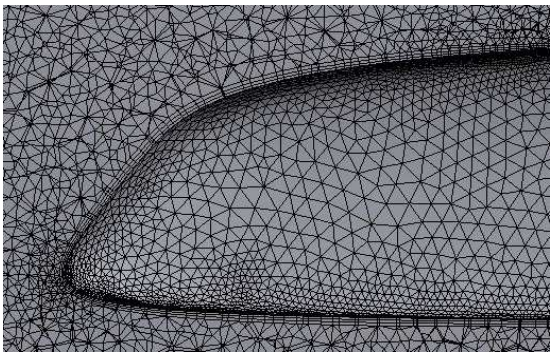

Figure 4. *Grid generated, front of the Impuls train.*

Table 3. *Mesh statistics.*

Name of train	Number of nodes	Number of elements
Pendolino ED250	722 580	3 134 085
Impuls 45WE	746 919	3 300 352

Two parameters are used to compare quality of meshes. The skewness is the angular measure of element quality with respect to the angles of ideal element types. The element quality compounds three another mesh features: orthogonal quality, aspect ratio and skewness.

Table 4. *Mesh metrics.*

Name of train	Average skewness	Average element quality
Pendolino ED250	0.2118	0.8268
Impuls 45WE	0.2130	0.8229

3.3. Boundary conditions and fluid properties

Types of boundary conditions used in this simulation:

- on the front surface - velocity inlet,
- on the rear surface - pressure outlet,
- on the train faces and bottom surface - wall,
- on the top and sides surfaces- symmetry.

Velocity must be defined by vector with correct magnitude and with correct direction. Wall boundary conditions are used to bound fluid off solid regions.The shear stress and heat transfer between the fluid and wall are computed based on the flow details in the local flow field.When all surfaces around domain are walls, then it will be a simulation of train, which moves in tunnel. Symmetry boundary conditions are used when the physical geometry of interest, and the expected pattern of the flow/thermal solution, have mirror symmetry. They can also be used to model zero-shear slip walls in viscous flows.Velocity inlet boundary conditions are used to define the flow velocity, along with all relevant scalar properties of the flow, at flow inlets.This boundary condition is intended for incompressible flows, and its use in compressible flows will lead to a nonphysical result because it allows stagnation conditions to float to any level. Pressure outlet boundary conditions require the specification of a static (gauge) pressure at the outlet boundary. The value of the specified static pressure is used only while the flow is subsonic.When the flow becomes locally supersonic, the specified pressure will no longer be used; pressure will be extrapolated from the flow in the interior. All other flow quantities are extrapolated from the interior.

Each calculation was carried out with constant gas density, because it is necessary to fix the mass flow.

3.4. Turbulent models comparison

This analysis was simulated for following assumptions:

- inlet velocity – 50 (m/s),
- first order upwind.

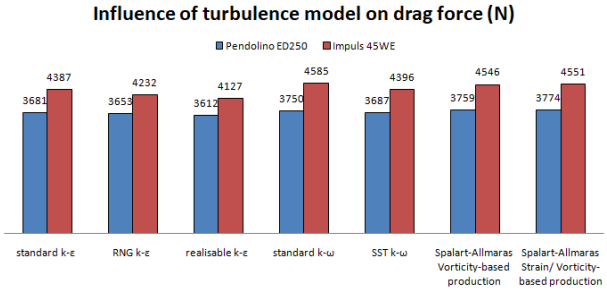

Figure 7. *Bar graph of analysed drag force versus turbulence model.*

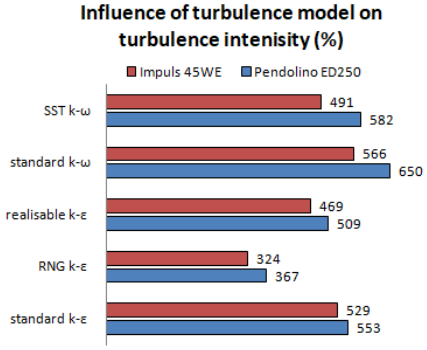

Figure 8. *Bar diagram of analysed turbulence intensity versus two equations turbulence model.*

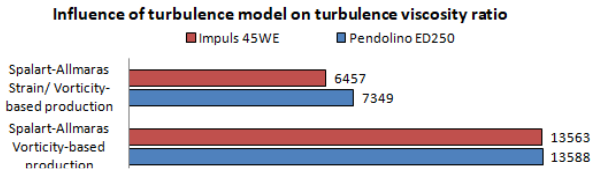

Figure 9. *Bar diagram of analysed turbulence viscosity ratio versus one equation turbulence model.*

The difference between turbulence viscosity ratio of both train models applied by Spalart-Allmaras models arises from the different values of coefficients, which are used to solve equation.

3.5. Discretisation methods

The solution methods for turbulence kinetic energy, turbulence dissipation ratio, modified turbulence ratio and turbulence dissipation frequency are:

- First order upwind,
- Second order upwind.

First-order accuracy is desired, when quantities at cell faces are determined by assuming that the cell-center values of any field variable represent a cell-average value and hold throughout the entire cell. In second order upwind, higher-order accuracy is achieved at cell faces through a Taylor series expansion of the cell-centered solution about the cell centroid. The influence of discretisation methods are compared on the bar graphs for both cases. This scrutiny was created for following assumptions:

- inlet velocity – 50 (m/s),
- standard k-ε model.

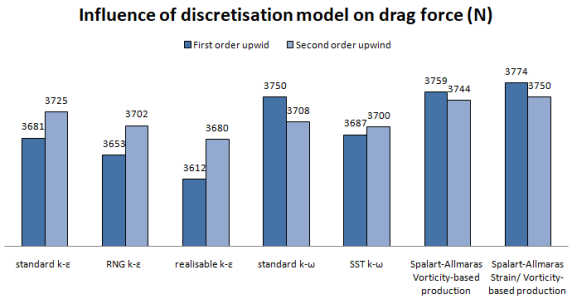

Figure 5. *Bar graph of analysed drag force versus discretisation model for Pendolino ED250.*

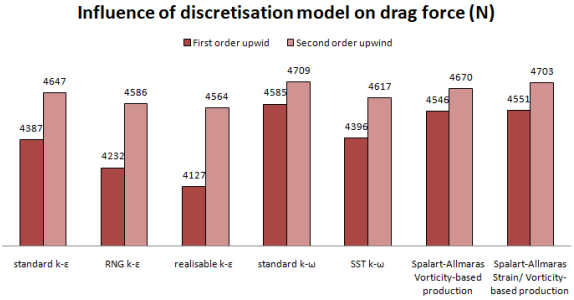

Figure 6. *Bar graph of analysed drag force versus discretisation model for Impuls 45WE.*

The maximum relative error between drag force for various turbulence models for Pendolino is at rough estimate:

- 2.5% (first order upwind),
- 1.0% (second order upwind).

Thus the choice of turbulence model has less influence on the results when parameters are solved by using second order upwind.

The values of Impuls drag force varies from the mean drag force for about 6.3% for first order upwind and for about 1.6% for second order upwind. This errors may be generated by lower mesh quality in the case of Impuls model.

3.5. Aerodynamic comparison

The pictures below present the distribution of air pressure and turbulent kinetic energy around the trains for following conditions:

- first order upwind – discretisation method,
- standard k-ε – turbulence model,
- inlet velocity - 50 (m/s).

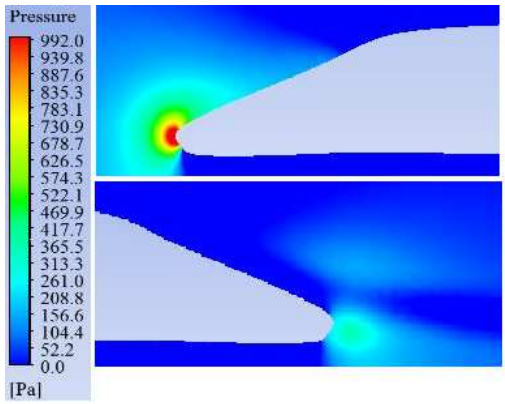

Figure 10.*Air pressure distribution in front and behind train – Pendolino ED250.*

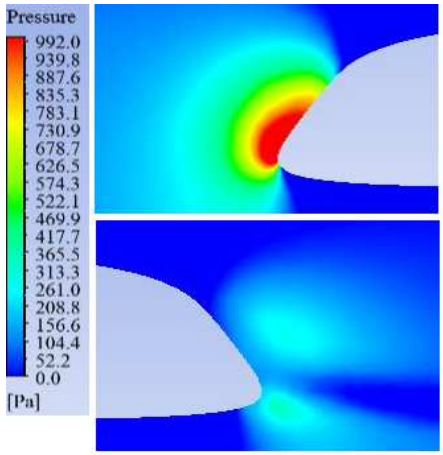

Figure 11. *Air pressure distribution in front and behind train – Impuls 45WE.*

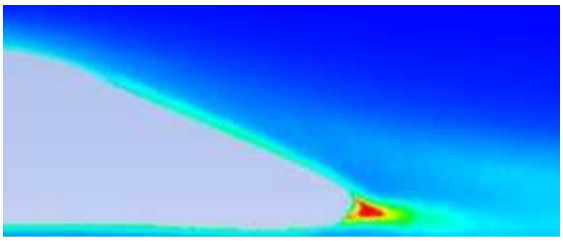

Figure 12. *Turbulent kinetic energy distribution behind train – Pendolino ED250.*

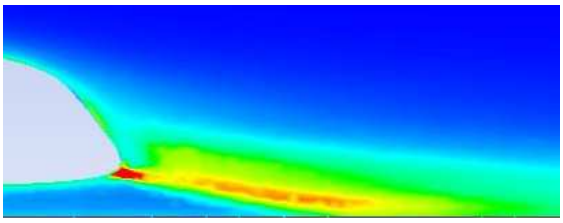

Figure 13. *Turbulent kinetic energy distribution behind train – Impuls 45WE.*

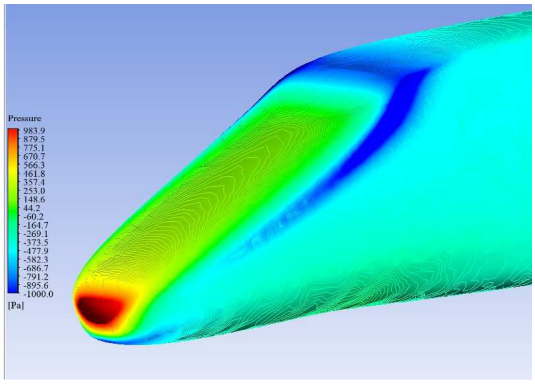

Figure 14. *Pressure distribution on the head of the train – Pendolino ED250.*

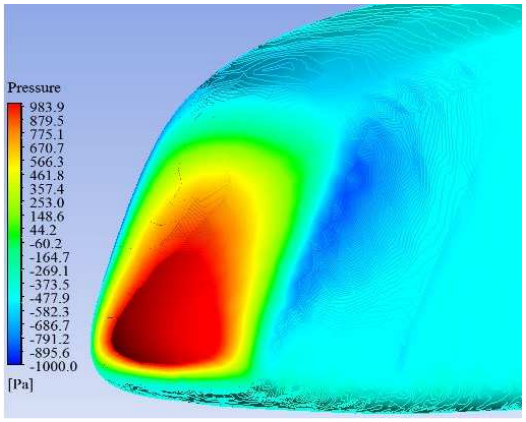

Figure 14. *Pressure distribution on the head of the train – Impuls 45WE.*

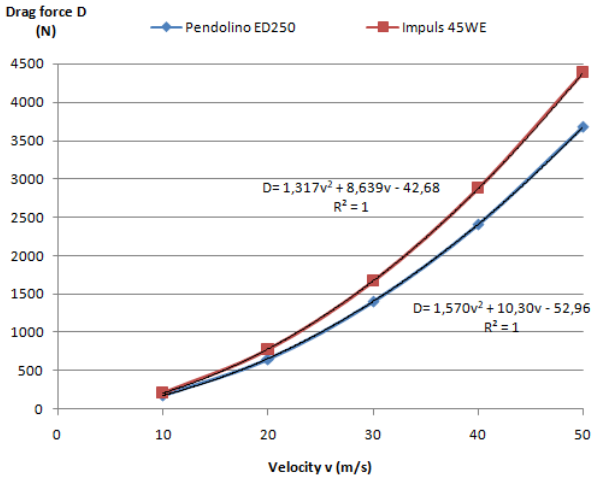

Figure 16. *Plot of analysed drag force versus inlet velocity.*

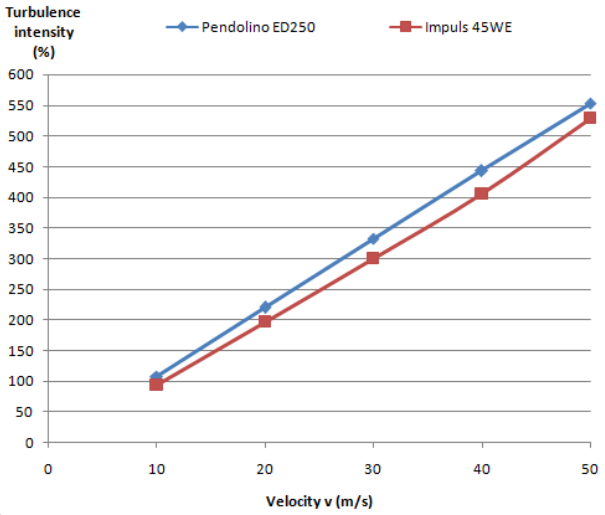

Figure 17. *Plot of analysed turbulence intensity versus inlet velocity.*

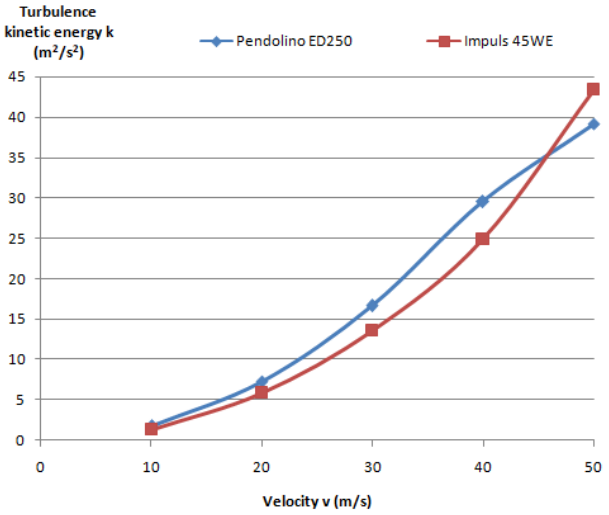

Figure 18. *Plot of analysed turbulence kinetic energy versus train velocity.*

3.6. Discussion

We can see that aerodynamic comparison of two train models lead us to the conclusion that Pendolino ED250 generates less drag force than Impuls 45WE for every turbulence models and discretisation models. The difference in drag force rises when value of air particles velocity goes up according to figure 16. Thus drag coefficient for geometry based on Impuls 45WE is greater than this parameter for the second train model. The value of turbulence intensity goes up steadily in the function of inlet velocity for both cases. The results from second order upwind gives greater value of drag force in comparison to the results for first order upwind. The relative errors of drag force have less value in case of simulation with second order upwind so the simplest turbulence models give accurate solution. In accordance with formula (2), drag force of Impuls 45WE is average 19% bigger than drag force of Pendolino ED250 for change velocity from 10 to 50 m/s, because the first train has greater value of drag coefficient.

4.Concluding information

The drag force is important factor which has an effect on energy consumption of aerodynamic vehicles. In this paper a verification of turbulence models and discretisation models were presented. First order upwind and second order upwind were used to compare. This analyse was realized using three turbulence models: Spalart-Allmaras, k-ε and k-ω. Both trains have the same boundary conditions and the domain geometries. The results obtained were: drag force, turbulence intensity, turbulent viscosity ratio, the relationship between them and velocity inlet. Pressure and turbulent kinetic energy distribution were presented by using contours. Others parameters on the diagram bars and plots. The main dimension of trains are similar so the drag force depends on the front and the rear shape of vehicles.

Symbols

ω turbulence frequency (1/s),
ε turbulence dissipation rate (m^2/s^3),
k turbulent kinetic energy (m^2/s^2),
D drag force (N),
P_d dynamic pressure (N/m^2),
A reference area (m^2),
C_d drag coefficient (-),
I turbulence intensity (-),
$u`$ turbulent velocity fluctuation (m/s),
U mean velocity (m/s),
U_x, U_y, U_z mean velocity components (m/s),

References

[1] P. Spalart and S. Allmaras.
*A one-equation turbulence model for aerodynamic flows.*Technical Report AIAA-92-0439, American Institute of Aeronautics and Astronautics, 1992.

[2] B. E. Launder and D. B. Spalding.
Lectures in Mathematical Models of Turbulence.
Academic Press, London, England, 1972.

[3] V. Yakhot and S. A. Orszag.
Renormalization Group Analysis of Turbulence: I. Basic Theory.
Journal of Scientific Computing, 1(1):1-51, 1986.

[4] T.-H. Shih, W. W. Liou, A. Shabbir, Z. Yang, and J. Zhu.
A New k-ε Eddy-Viscosity Model for High Reynolds Number Turbulent Flows - Model Development and Validation.
Computers Fluid*s*, 24(3):227-238, 1995.

[5] D. C. Wilcox.
Turbulence Modeling for CFD.
DCW Industries, Inc., La Canada, California, 1998.

[6] F. R. Menter.
Two-Equation Eddy-Viscosity Turbulence Models for Engineering Applications.
AIAA Journal, 32(8):1598-1605, August 1994.